Open Ceramics 26 (2026) 100980

Contents lists available at ScienceDirect

Open Ceramics

journal homepage: www.sciencedirect.com/journal/open-ceramics

Effects of airborne-particle abrasion and zirconia composition on porcelain–zirconia bond strength

Maja Antanasova [a], Tine Malgaj [b,*], Sandra Drev [c], Milan Vukšić [a], Peter Jevnikar [b], Andraž Kocjan [a]

[a] Jožef Stefan Institute, Department for Nanostructured Materials, Jamova 39, 1000 Ljubljana, Slovenia
[b] University of Ljubljana, Faculty of Medicine, Department of Prosthodontics, Hrvatski trg 6, 1000 Ljubljana, Slovenia
[c] Jožef Stefan Institute, Center for Electron Microscopy and Microanalysis, Jamova 39, 1000 Ljubljana, Slovenia

ARTICLE INFO

Keywords:
Airborne-particle abrasion
Yttria-stabilized zirconia (Y-TZP)
Zirconia-based ceramics
Porcelain–zirconia interface
Bond strength
Surface treatment

ABSTRACT

Porcelain chipping in zirconia-based dental restorations remains a major clinical complication. This study evaluated the effects of airborne-particle abrasion (APA) and yttria content in zirconia on porcelain–zirconia bond strength. Six groups were tested: low-translucency (3Y-TZP) and high-translucency zirconia (4Y-TZP), each with or without APA, and APA-treated Co–Cr and Ti–6Al–4V alloys as metal–ceramic references. Bond strength was assessed using the Schwickerath test. Interfacial structure and mechanical properties were analyzed by scanning and transmission electron microscopy and nanoindentation. APA significantly increased zirconia surface roughness but did not improve bond strength. Zirconia composition had no effect on porcelain bonding. Bond strength values for porcelain-zirconia (34.0–40.6 MPa) were comparable to those of metal–ceramic systems, lower than Co–Cr (45.5 MPa) but similar to Ti–6Al–4V (37.3 MPa). Microscopy and nanoindentation revealed sharp zirconia–porcelain interfaces with pronounced mechanical mismatch and yttrium segregation at grain boundaries.

1. Introduction

An ideal dental material combines superior mechanical performance—high flexural strength, fracture toughness, and resistance to crack propagation under functional and parafunctional loads—with excellent aesthetic qualities, including natural tooth coloration and optimal light translucency. However, the mechanical performance of dental materials and their aesthetic appearance seem to be inversely correlated. Feldspathic dental porcelains offer excellent aesthetics, biocompatibility, and resistance to compressive forces; however, their low tensile strength makes them prone to fracture under shear or tensile loads [1]. Highly aesthetic feldspathic porcelains are thus combined with high-strength dental materials like metal alloys and zirconia-based ceramics to meet both mechanical and aesthetic requirements for prosthetic restorations.

The success of fixed dental prostheses (FDPs) and other indirect restorations critically depends on the reliable bonding of veneering porcelain to the underlying substrate. Metal–ceramic systems have long been considered the gold standard due to their predictable mechanical performance and durable chemical bonding through oxide layers formed on the metal surface [2–4]. Cobalt–chromium (Co–Cr) alloys, in particular, exhibit high bond strength with porcelain, facilitated by micromechanical interlocking and chemical bonding at the oxide–ceramic interface [5]. In contrast, titanium-based alloys, such as Ti-6Al-4V, present challenges for porcelain veneering due to the formation of thick, brittle oxide layers and a high affinity for oxygen, which can compromise interfacial bonding [6,7].

Zirconia-based ceramics have emerged as a widely used alternative to metal frameworks in modern restorative dentistry due to their high strength, biocompatibility, and favorable aesthetics [8,9]. Yttria-stabilized tetragonal zirconia polycrystals (Y-TZP) are the most

Abbreviations: APA, Airborne-particle abrasion; AM, As-milled; CTE, Coefficient of thermal expansion; EDS, Energy-dispersive spectroscopy; E_M, Young's modulus of elasticity; FDP(s), Fixed dental prosthesis/prostheses; FE-SEM, Field-emission scanning electron microscopy; HAADF, High-angle annular dark-field; ISO, International organization for standardization; R_a, Average surface roughness; SEM, Scanning electron microscopy; STEM, Scanning transmission electron microscopy; TEM, Transmission electron microscopy; Y-TZP, Yttria-stabilized tetragonal zirconia polycrystals; 3Y-TZP, 3 mol% yttria-stabilized tetragonal zirconia polycrystals; 4Y-TZP, 4 mol% yttria-stabilized tetragonal zirconia polycrystals.

* Corresponding author.
E-mail address: tine.malgaj@mf.uni-lj.si (T. Malgaj).

https://doi.org/10.1016/j.oceram.2026.100980
Received 20 March 2026; Received in revised form 24 April 2026; Accepted 12 May 2026
Available online 12 May 2026

commonly used variants, with 3 mol% yttria (3Y-TZP) providing high strength and low translucency, while higher yttria contents (4Y-TZP, 5Y-TZP) increase translucency at the cost of reduced fracture toughness [10–14]. To achieve the best aesthetic results and natural appearance, zirconia-based ceramics are often combined with glaze [15] or feldspathic porcelain. However, zirconia is chemically inert and lacks a silica-based glass phase, limiting its ability to chemically bond to feldspathic porcelain. As a result, mechanical retention and interfacial compatibility become the primary determinants of bond performance [16].

Surface treatments, such as airborne-particle abrasion (APA), are commonly employed to enhance substrate roughness and promote micromechanical interlocking with veneering porcelain. While APA has been shown to significantly improve bond strength in metal–ceramic systems [17,18], its effect on zirconia is less straightforward. APA can induce surface roughening, leading to enhanced porcelain bonding [16], but also generates surface defects and phase transformations [19,20], which may negatively affect interfacial integrity and bond durability [21,22]. Moreover, the impact of zirconia composition, specifically yttria content, on porcelain bonding remains incompletely understood. Recent studies suggest that differences in phase composition and mechanical behavior between 3Y-TZP and 4Y-TZP may influence surface response to APA, but their clinical significance for veneering porcelain remains unclear [10,23].

Clinical outcomes from long-term evaluations of FDPs indicate that zirconia-based restorations can achieve high survival rates similar to conventional metal–ceramic systems, even though differences in technical complications, especially veneering ceramic chipping, have been observed. In a randomized clinical trial of three-unit posterior FDPs, zirconia and metal–ceramic restorations exhibited equivalent 100% survival at 5 years, but zirconia was associated with a higher incidence of minor chipping (up to 20%) despite similar periodontal outcomes between the groups [24]. Retrospective data over 10 years showed comparable survival among high noble, Co–Cr, and zirconia FDPs, though metal systems demonstrated higher chipping-free survival and overall success rates, suggesting more stable veneering performance over longer service times [25]. Medium-term clinical assessments of zirconia vs metal–ceramic posterior FDPs have also reported similar survival rate, with only minor veneer chipping as the primary technical issue for zirconia [26]. Five-year survival rates of zirconia restorations frequently approximate those of metal-ceramics, though technical complications such as veneer fracture are more prevalent with ceramic frameworks [27]. These clinical findings highlight the need to better understand the material- and treatment-dependent factors that govern porcelain bonding and veneering reliability. Thus, a comprehensive understanding of the interplay between zirconia composition, surface treatment, and porcelain bond strength is essential.

Several studies have compared the bond strength of porcelain to metals versus zirconia. Metal–ceramic systems consistently show higher bond strength compared to zirconia–porcelain systems, under laboratory conditions [8,28,29]. Furthermore, bond strength testing in the literature has employed a variety of methods, including shear, micro-shear, and three-point bending tests, often resulting in incomparable outcomes due to differences in specimen geometry, loading conditions, and stress distributions. In this study, porcelain-to-substrate bond strength was evaluated according to the ISO 9693:2019 standard, which provides a rigorous, internationally recognized framework for compatibility testing of metal–ceramic and ceramic–ceramic systems [30].

The main goal of the study was to achieve a more reliable comparative assessment of the influence of the substrate material on the bond strength in both metal-ceramic and ceramic-ceramic systems. In addition, the effects of APA and zirconia composition (3Y-TZP vs. 4Y-TZP) on surface roughness and porcelain bond strength were investigated. Detailed microstructural and mechanical characterization of the interfaces was also performed to better understand the underlying mechanisms of porcelain–zirconia adhesion.

2. Materials and methods

Rectangular CAD specimens were designed using exocad DentalCAD software (exocad GmbH, Darmstadt, Germany) according to the dimensional requirements of ISO 9693:2019. Six experimental groups were defined based on substrate material and surface treatment. The zirconia groups (n = 12 specimens per group) consisted of high-translucency zirconia (4Y-TZP) and low-translucency zirconia (3Y-TZP), each prepared with or without APA. The metal reference groups (n = 10 specimens per group) were APA-treated cobalt–chromium (Co-Cr) and titanium (Ti-6Al-4V) alloys. Chemical compositions and materials properties are listed in Table 1.

Zirconia substrates were fabricated by CNC milling using a Ceramill micro unit (Amann Girrbach GmbH, Pforzheim, Germany) and subsequently sintered at 1450 °C for 2 h with a heating rate of 8 °C/min in a Ceramill Therm furnace (Amann Girrbach GmbH). Co-Cr and Ti-6Al-4V substrates were produced by CNC milling using an Arrow Mill Beluga unit (DENTAS l.l.c., Maribor, Slovenia). All specimens were manufactured to final dimensions of 25 × 3 × 0.5 mm, in compliance with ISO 9693:2019 standard.

Surface preparation was performed as follows. Zirconia groups (3Y-TZP, 4Y-TZP) were left as-milled, or airborne-particle abraded with 50 μm Al_2O_3 particles (Korox; BEGO GmbH & Co. KG, Bremen, Germany). Co–Cr and Ti-6Al-4V specimens were airborne-particle abraded with 110 μm Al_2O_3 particles (Korox; BEGO GmbH & Co. KG, Bremen, Germany). The alumina particle size was determined according to previous data [17,21,31–33]. All APA procedures were carried out for 10 s at a pressure of 0.2 MPa and a 45° incidence angle. All specimens were subsequently steam-cleaned and allowed to dry. An overview of the experimental groups is provided in Table 1.

Surface roughness characterization was conducted on randomly selected specimens from each group before porcelain application. Three profilometric measurements, each 3 mm in length, were obtained using a contact profilometer (Talysurf 10; Taylor Hobson Ltd., Leicester, UK), and the average surface roughness (R_a) values were calculated for each group.

Feldspathic porcelain was applied centrally to each substrate over an area measuring 8 mm in length, 3 mm in width, and 1.1 mm in thickness, in accordance with ISO 9693:2019 (Fig. 1). To minimize handling variability and ensure consistent porcelain geometry, all specimens were positioned in a custom-designed stainless-steel holder during porcelain application. In accordance with manufacturer guidelines and established clinical protocols, different veneering porcelains were used for Co–Cr, Ti–6Al–4V, and zirconia to ensure substrate-specific compatibility in the coefficient of thermal expansion (CTE) and firing conditions, minimizing interfacial residual stresses and the risk of veneer failure [34,35]. A fine-structure feldspathic porcelain adapted to zirconia frameworks (VITA VM9; VITA Zahnfabrik, Bad Säckingen, Germany) was applied to both 3Y-TZP and 4Y-TZP zirconia substrates. A base dentin wash-bake was performed, followed by two dentin porcelain layers and a final glaze firing. For Co-Cr substrates, a conventional low-fusing feldspathic porcelain (VITA VMK Master; VITA Zahnfabrik) was used, while Ti-6Al-4V substrates received an ultra-low-fusing porcelain formulated for titanium (Ceramotion Ti; Dentaurum, Ispringen, Germany), with adjusted firing temperatures and a reduced coefficient of thermal expansion to match titanium. For the metal groups, a wash paste (Co-Cr) or bonding agent (Ti-6Al-4V) was applied and fired prior to the opaque layer, followed by two dentin layers (with the second compensating for firing shrinkage) and glaze firing. All porcelain firings were carried out in a Vita Vacumat 6000 M furnace (VITA Zahnfabrik) using firing schedules recommended by the manufacturers.

For each zirconia experimental group, 12 specimens were prepared. Ten porcelain–zirconia specimens were used for bond strength testing. The remaining specimens in each group were assigned to additional

Table 1
Specification of groups and substrate materials used in this study.

Substrate	Material type	General composition of the substrate [wt %] [a]	CTE [a, b] [x10^{-6} K^{-1}]	E_M [GPa] [a]	Brand name and manufacturer	Surface preparation	Group
Co-Cr	Co-Cr alloy (milling blank)	Co (60.5), Cr (28), W (9), Si (1.5), Other: Mn, N, Nb, Fe (< 1%)	14.1	230	Remanium Star MD I (Dentaurum GmbH & Co. KG, Ispringen, Germany)	APA	**Co-Cr APA**
Ti-6Al-4V	Ti-6Al-4V alloy (milling blank)	Ti-6Al-4V alloy: Ti (>90), Al (5.5–6.75), V (3.5–4.5), Other (<0.4)	10.3	110	Zanotec Ti (Wieland Dental + Technik GmbH & Co KG, Pforzheim, Germany)	APA	**Ti-6Al-4V APA**
3Y-TZP	Low translucent zirconia oxide (pre-sintered blanks)	$ZrO_2 + HfO_2 + Y_2O_3$ (≥ 99), Y_2O_3 (4.5 – 5.6), HfO_2 (≤ 5), Al_2O_3 (≤ 0.5), $SiO_2 + Fe_2O_3$ < 0.5	10.4 ± 0.5	≥ 200	Ceramill Zi white (Amann Girrbach GmbH, Pforzheim, Germany	AM	**3Y-TZP AM**
						APA	**3Y-TZP APA**
4Y-TZP	Highly translucent zirconia oxide (pre-sintered blanks)	ZrO2 + $HfO_2 + Y_2O_3$ (≥ 99), Y_2O_3 (6.7 – 7.2), HfO_2 (≤ 5), Al_2O_3 (≤ 0.5), Other oxides (≤ 1)	10.4 ± 0.5	≥ 200	Ceramill Zolid HT+ white (Amann Girrbach GmbH, Pforzheim, Germany)	AM	**4Y-TZP AM**
						APA	**4Y-TZP APA**

Abbreviations: CTE – Coefficient of Thermal Expansion; E_M- Young's modulus of elasticity, APA – airborne-particle abrasion, AM – As-milled.
[a] As provided by the manufacturer.
[b] In the range 25–500 °C.

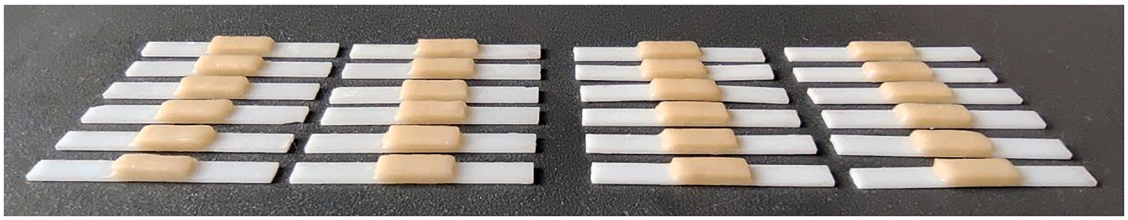

Fig. 1. The zirconia–porcelain specimens were prepared in accordance with ISO 9693:2019.

analyses: one randomly selected specimen per group was used for mechanical and microstructural characterization of the interface by nanoindentation and field-emission scanning electron microscopy (FE-SEM), and one randomly selected specimen per group was used for further transmission electron microscopy (TEM) analyses. All metal–ceramic specimens (n = 10 per group) were subjected to bond strength testing.

Porcelain–substrate bond strength was evaluated using the Schwickerath crack-initiation three-point bending test in accordance with ISO 9693:2019 [30]. Specimens were supported over a 20 mm span and loaded with a 2 mm-diameter piston at a crosshead speed of 1.5 mm/min in a universal testing machine (Instron 4301; Instron Corp., Norwood, MA, USA) until crack initiation occurred (Fig. 2). The maximum load prior to a sudden drop in the load–deflection curve was recorded as the debonding force (F). Flexural bond strength values (MPa) were calculated using the ISO-prescribed equation$\tau b = F \times k$, with the coefficient k determined based on substrate thickness (0.5 ± 0.05 mm) and Young's modulus of elasticity, as specified in ISO 9693.

For the zirconia specimens, in addition to macroscopic bond strength testing, local mechanical properties across the porcelain–substrate interface were assessed by nanoindentation. Measurements were performed using a Hysitron TI/TS-140 nanoindenter (Bruker, Minneapolis, MN, USA) equipped with a Berkovich diamond tip and operated in fast XPM (accelerated property mapping) mode. Due to the rapid acquisition of XPM, a smaller scanned area and reduced indentation spacing were used compared to conventional grid-based nanoindentation.

The interface regions of the prepared cross-sectioned specimens were scanned over an area of 36 × 36 μm using the scanning capability of the indenter transducer. A grid of 19 × 19 indents with an inter-indent spacing of 2 μm was selected to minimize interaction effects between adjacent indentations. Nanoindentation measurements were conducted directly across the porcelain–substrate interface by applying a maximum load of 5 mN. The loading protocol consisted of linear loading for 0.1 s,

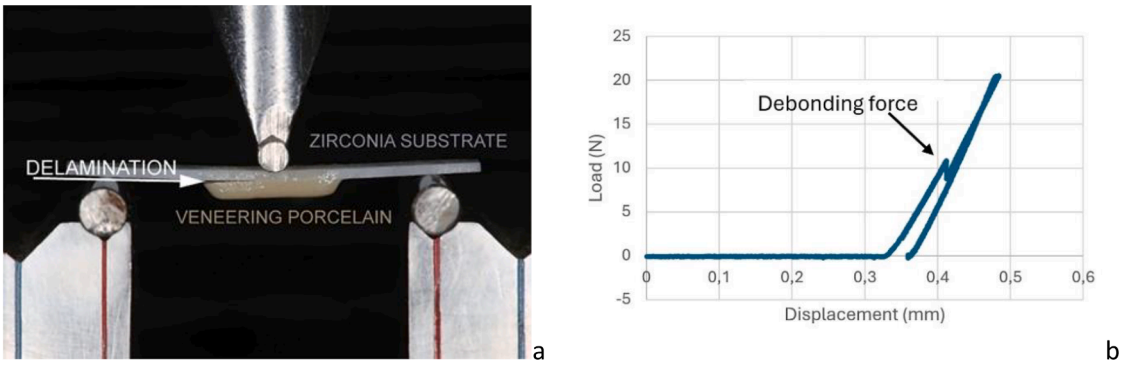

Fig. 2. (a) The porcelain-to-metal and porcelain-to-zirconia ceramics bond strengths were assessed with the Schwickerath crack-initiation three-point bending test, as recommended by ISO 9693:2019; (b) load–deflection curve assessing the debonding force as a first maximal load prior to a sudden drop.

followed by a 0.1 s holding segment, and linear unloading over 0.1 s. The resulting load–displacement data were used to assess spatial variations in mechanical properties across the interface.

Interfacial morphology and elemental distribution were examined using field-emission scanning electron microscopy (FE-SEM; Jeol JSM-7600F, Jeol Ltd., USA) coupled with energy-dispersive spectroscopy (EDS) line scans (22 μm length, 15 kV accelerating voltage, 15 mm working distance).

Additional transmission electron microscopy (TEM) combined with EDS analyses was conducted to further characterize the elemental distribution across the porcelain–zirconia interface. For bulk TEM analysis, selected zirconia samples were sectioned into 1.8 × 1.8 mm blocks and mounted in 3 mm brass holders using epoxy resin. Specimens were mechanically thinned to approximately 100 μm, dimpled to ~15 μm at the center, and finally ion-milled (PIPS; Gatan Inc., USA) using 3 kV Ar^+ ions at an 8° incidence angle until perforation.

Scanning TEM (STEM) was performed using a probe-corrected Spectra 300 S/TEM (Thermo Fisher Scientific, Waltham, MA, USA) operated at 200 kV. High-angle annular dark-field (HAADF) and bright-field images were acquired, and elemental mapping was conducted using energy-dispersive spectroscopy. Data acquisition and post-processing were carried out using Velox software (v. 3.15).

Statistical analyses of bond strength and surface roughness data were performed using SPSS Statistics version 22 (IBM Corp., NY, USA). Data normality and homogeneity of variance were assessed using the Shapiro–Wilk and Levene tests, respectively. One-way ANOVA, followed by Tukey's HSD post hoc test, was employed to evaluate the effects of different substrates on surface roughness and their bond strength with porcelain. The significance level was set at $\alpha = 0.05$. In addition, a two-way ANOVA was performed for zirconia specimens to assess the effects of zirconia composition (3Y-TZP vs. 4Y-TZP) and surface treatment (APA vs. no APA), as well as their interaction, on surface roughness and porcelain–zirconia bond strength.

3. Results

Mean surface roughness values (R_a) and porcelain-to-substrate bond strength values for all experimental groups are summarized in Table 2. One-way ANOVA revealed significant differences in surface roughness among the substrate groups ($F_{(5,12)} = 45.54$, $p < 0.001$). The metal alloys (Co–Cr and Ti-6Al-4V) exhibited significantly higher R_a values than the zirconia ceramics, regardless of zirconia composition or surface treatment. Among zirconia substrates, APA significantly increased surface roughness compared with untreated surfaces.

Two-way ANOVA performed on the four zirconia groups revealed statistical differences ($F_{(3,\ 8)} = 9.77$, $p = 0.005$). APA had a highly significant effect on surface roughness ($p = 0.001$). In contrast, zirconia composition (3Y-TZP vs. 4Y-TZP) did not significantly influence R_a ($p = 0.189$). The interaction between APA and zirconia composition was also not significant ($p = 0.826$), indicating that the roughening effect of APA was consistent across both zirconia compositions.

One-way ANOVA revealed a significant effect of substrate type on porcelain-to-substrate bond strength ($F_{(5,54)} = 4.58$, $p = 0.001$). Post hoc comparisons using Tukey's HSD test identified distinct statistical groupings among the experimental conditions (Table 2). Co–Cr substrates exhibited the highest bond strength values, with no significant differences compared to as-milled zirconia substrates (3Y-TZP and 4Y-TZP). Bond strength values for as-milled zirconia fell between those of Co–Cr and Ti-6Al-4V, although the differences were not statistically significant. In contrast, APA-treated zirconia and Ti-6Al-4V substrates exhibited significantly lower bond strength values than Co–Cr.

The two-way ANOVA model evaluating the effects of zirconia composition (3Y-TZP vs. 4Y-TZP) and surface treatment (APA vs. no APA), as well as their interaction, on porcelain–zirconia bond strength was not statistically significant ($F_{(3,\ 36)} = 2.10$, $p = 0.118$). Furthermore, neither the main effect of zirconia composition ($p = 0.241$) nor the interaction between APA and composition ($p = 0.796$) reached statistical significance. Although the main effect of APA yielded a significant p-value ($p = 0.035$), this result should be interpreted with caution given the non-significant overall model. Numerically, slightly lower bond strength values were observed following APA (3Y-TZP: 38.75 → 34.01 MPa; 4Y-TZP: 40.55 → 36.82 MPa).

Young's modulus and hardness, measured by nanoindentation, revealed pronounced differences between the zirconia substrates and the porcelain layer. The microstructure image shows that the porcelain has thoroughly wetted the surface (Fig. 3). The interface appears continuous and uniform, with no visible voids or lunkers. There were no signs of porosity, gaps, or interfacial defects, indicating intimate contact between the porcelain and the substrate. Zirconia exhibited substantially higher stiffness, with Young's modulus values of approximately 200 GPa, as well as higher hardness compared with the overlying porcelain. These trends were consistent for both zirconia compositions and surface treatments.

Representative SEM micrographs and EDS line-scan profiles of the porcelain–zirconia interfaces are shown in Fig. 4. All specimens exhibited continuous, pore-free interfaces without evidence of interfacial cracking or delamination. EDS line profiles revealed a gradual, but relatively sharp elemental transition from zirconia to porcelain, characterized by decreasing Zr and Y signal intensities toward the porcelain and a concomitant increase in Si, O, and Al signals. Important to note is difference in concentration of Al and Si within the bulk of zirconia. According to the manufacturer, Al_2O_3 content is ≤ 0.5 wt% (Table 1), which means the content of Si is even higher. The resulting sigmoidal intensity–distance profiles indicate a chemically well-defined but continuous interface.

STEM–EDS analysis (Fig. 5) provided higher-resolution insight into elemental distribution across the interface. Zirconium was confined to the zirconia substrate and was uniformly distributed within individual zirconia grains, consistent with the polycrystalline nature of the material. In contrast, yttrium exhibited a non-uniform distribution, with enrichment at grain boundaries and triple junctions. The porcelain layer was dominated by silicon-based phases. EDS line profiles confirmed a relatively sharp transition between zirconia and porcelain, with decreasing Zr and Y signals and increasing Si and Al signals toward the porcelain. As observed in Fig. 4, the amount of Si in the zirconia bulk is significantly higher (up to 10-times) than that of Al.

Table 2
Mean values and standard deviations for the surface roughness [R_a] of different substrates, together with porcelain-to-metal and porcelain-to-zirconia ceramics bond strengths.

Group	Substrate preparation	R_a (μm), n = 3/group	Bond strength (MPa), n = 10/group
Co-Cr APA	APA	1.05 ± 0.11^{a}	45.54 ± 6.07^{A}
Ti-6Al-4V APA	APA	1.27 ± 0.17^{a}	37.33 ± 4.12^{B}
3Y-TZP AM	AM	0.28 ± 0.07^{c}	$38.75 \pm 5.90^{A, B}$
3Y-TZP APA	APA	$0.50 \pm 0.06^{b, c}$	34.01 ± 6.10^{B}
4Y-TZP AM	AM	$0.34 \pm 0.09^{b, c}$	$40.55 \pm 7.91^{A, B}$
4Y-TZP APA	APA	0.57 ± 0.08^{b}	36.82 ± 3.80^{B}

Values marked with the same letters in the column do not differ significantly from each other (Tukey's HSD test, α=0.05).
APA – airborne-particle abrasion.
AM – as milled.
n – number of specimens.

4. Discussion

This study evaluated the effects of APA and zirconia composition on surface roughness and porcelain–zirconia bond strength. APA-treated zirconia exhibited lower bond strength than Co–Cr, whereas untreated

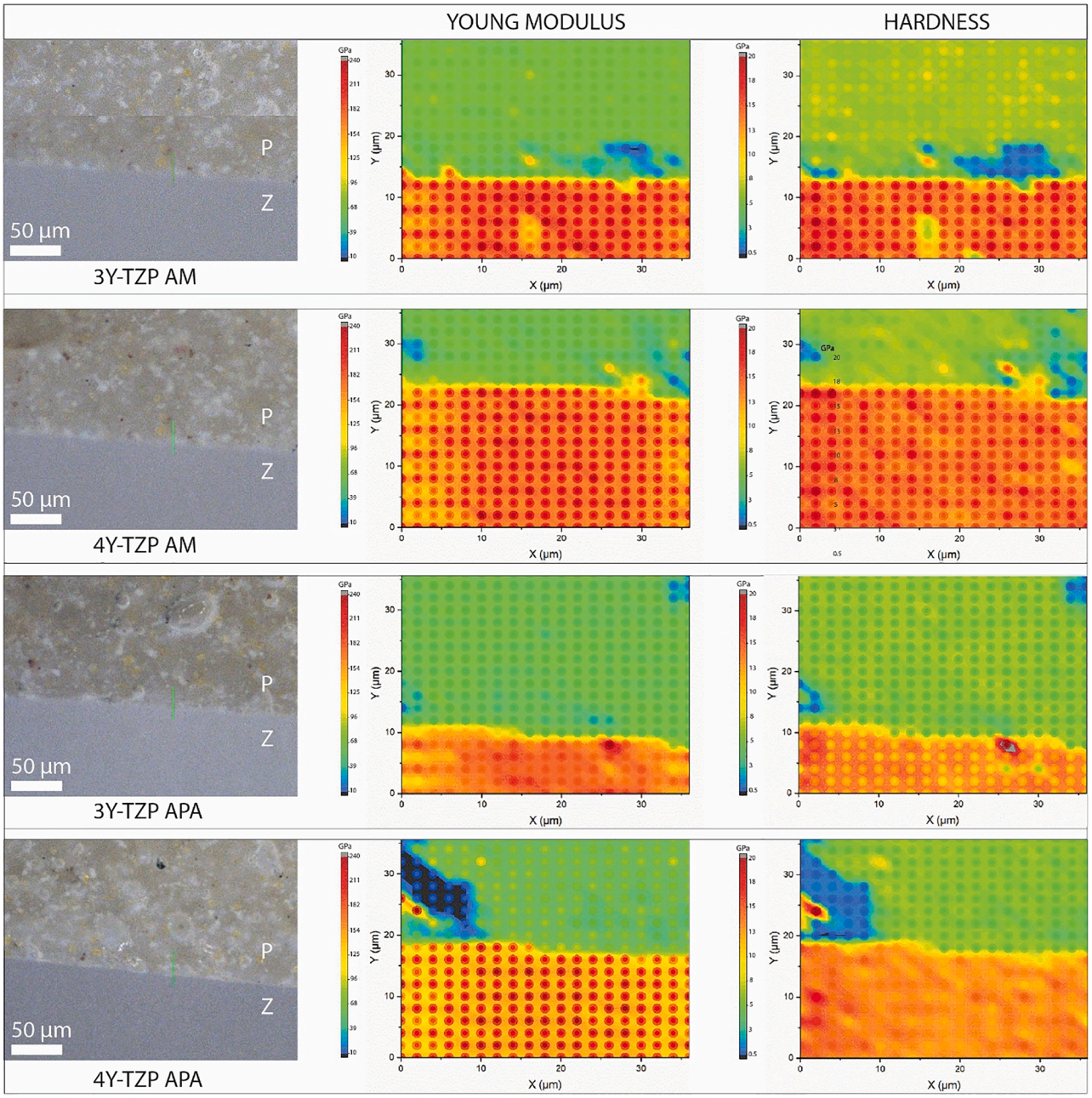

Fig. 3. Microstructural and nanomechanical characterization of zirconia–porcelain interfaces for untreated (AM) and airborne-particle abraded (APA) zirconia. In each row, the first image shows a representative optical micrograph of the interface, the second a Young's modulus map obtained by nanoindentation, and the third the corresponding hardness map. Rows correspond to 3Y-TZP AM, 4Y-TZP AM, 3Y-TZP APA, and 4Y-TZP APA. The micrographs show a continuous interface between porcelain (P) and zirconia (Z) without visible pores or voids. Zirconia exhibits higher Young's modulus (~150–240 GPa) and hardness (~12–20 GPa) than porcelain (~10–60 GPa and ~0.5–7 GPa, respectively), with a sharp mechanical transition across the interface and minor localized heterogeneities within the porcelain layer.

zirconia showed comparable bond strength to both metal substrates. APA significantly increased zirconia surface roughness but did not improve porcelain bond strength. Zirconia composition (3Y-TZP vs. 4Y-TZP) had no effect on porcelain bonding.

To provide a clinically relevant perspective on zirconia–porcelain bond strength, Co–Cr and Ti-6Al-4V alloys were included as reference substrates. Co–Cr alloys represent a well-established and clinically reliable substrate for porcelain veneering [2–4]. In contrast, porcelain bonding to titanium alloys is more challenging due to its high oxygen affinity and formation of thick, non-adherent oxide layers during firing, which can reduce the bond strength [6,36–38]. Accordingly, the Ti-6Al-4V group was therefore included as a comparative control representing a less favorable porcelain–metal bonding substrate.

APA is a well-established method for preparing metal substrates prior to porcelain veneering, as it increases surface roughness and promotes micromechanical interlocking at the metal–ceramic interface [17]. Accordingly, APA-treated Co–Cr and Ti-6Al-4V alloys were included in this study, in line with clinical practice and evidence showing that APA is essential for reliable porcelain–to-metal bonding [5,6,18,36]. APA Ti-6Al-4V showed higher surface roughness compared with APA Co–Cr, however, the difference did not reach statistical significance. This observation aligns with titanium's lower hardness and elastic modulus, which can promote increased plastic deformation under identical APA conditions and lead to more pronounced surface roughness [39,40]. Furthermore, titanium alloys form a relatively thick, brittle oxide layer on the surface that can crack or spall under blasting,

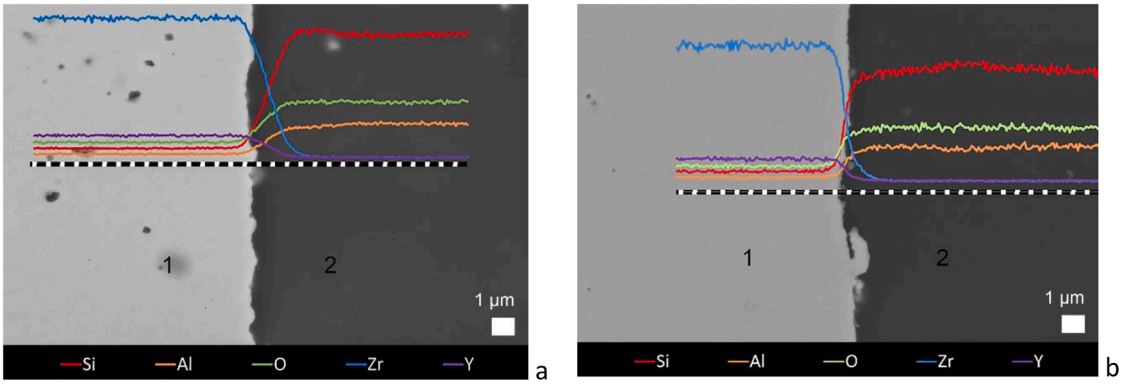

Fig. 4. SEM micrographs of the interfaces between dental porcelain and 3Y-TZP ceramics (a) or 4Y-TZP ceramics (b). Line-scan EDS profiles illustrate the variation in elemental composition from the zirconia substrate (1) to the porcelain layer (2). Curves of intensity (arbitrary units, counts per second) versus distance (μm) for each element are shown in different colors. The x- and y-axes have been omitted for clarity. The line scans provide qualitative information on the elemental distribution across the zirconia–porcelain interface.

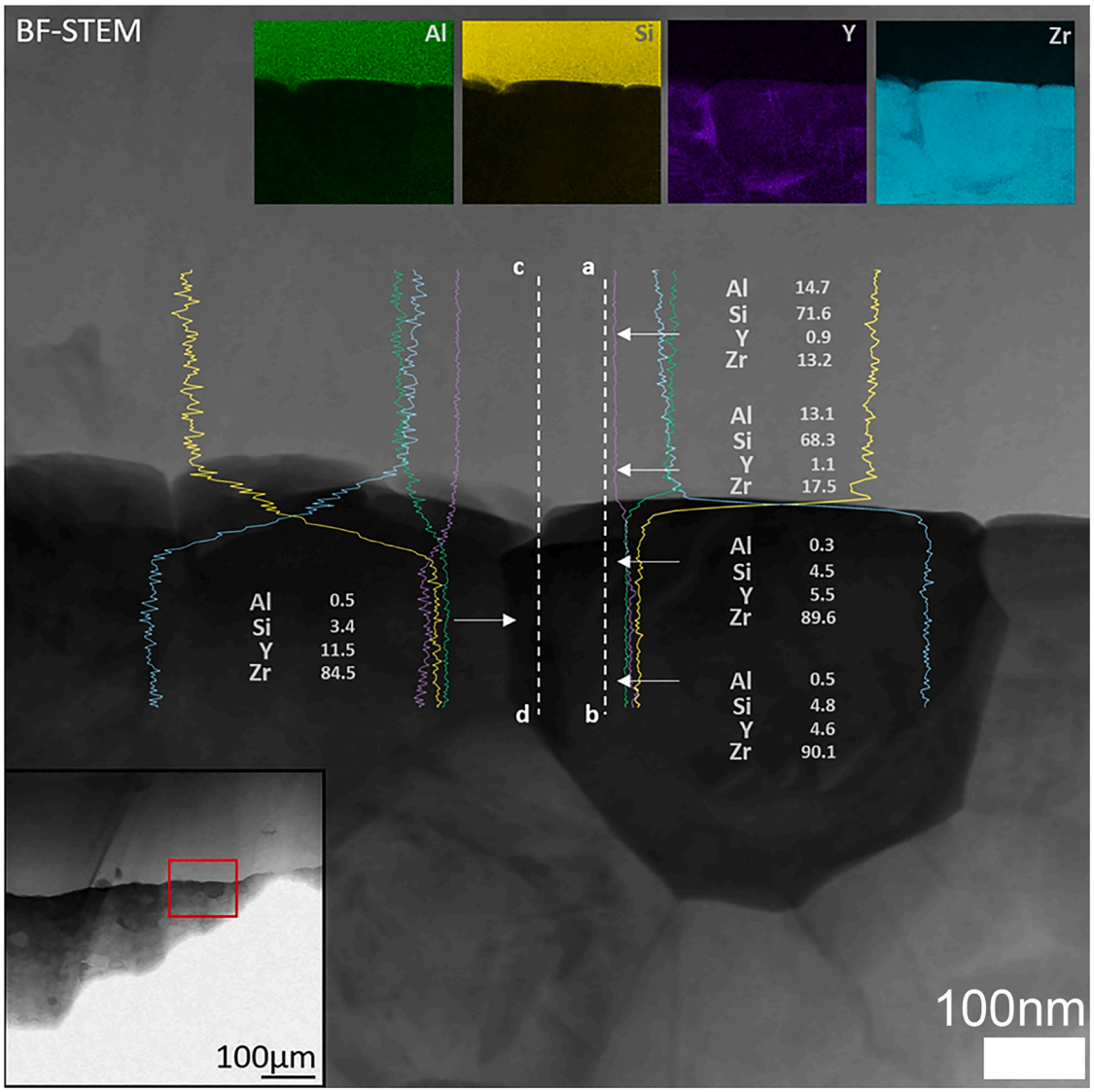

Fig. 5. STEM–EDS analysis provided higher-resolution insight into elemental distribution across the interface.

further increasing micro-pitting and surface roughness, while Co–Cr forms a harder, more adherent oxide that resists fracture and limits surface roughness [5,6].

When the APA protocol was applied to zirconia, the resulting surface

characteristics differed markedly. Both metal alloys exhibited substantially higher surface roughness than zirconia ceramics, irrespective of zirconia composition (3Y-TZP and 4Y-TZP) or surface treatment. Specifically, APA-treated Ti-6Al-4V and Co–Cr showed R_a values of 1.27 ± 0.17 μm and 1.05 ± 0.11 μm, respectively, whereas APA-treated zirconia reached only 0.50–0.57 μm. These differences could be related to the mechanical properties of the substrates. Namely, metals are more ductile than zirconia and deform plastically under abrasive impact, producing deeper surface grooves and higher roughness values, while zirconia is brittle and undergoes primarily micro-fracturing rather than plastic deformation during APA [5,41].

Furthermore, the particle size used in APA may confound differences in surface roughness. Metals were airborne-particle abraded with 110 μm Al_2O_3 particles in this study, whereas zirconia substrates were treated with smaller, 50 μm, particles, according to established evidence and clinical guidance [17,21,31–33,36]. Larger particles generate higher R_a values, particularly in ductile substrates such as Co–Cr and Ti-6Al-4V [42]. They also reduce residual alumina on the surface, enhancing micromechanical interlocking with porcelain [31]. Employing larger alumina particles appears to be beneficial for the metals, however, for zirconia, larger particles are reported to generate more pronounced stress-induced tetragonal to monoclinic phase transformation [8,9,21,32,33]. Specifically, monoclinic phase content has been reported to rise from 26% when abraded with 50 μm alumina to 40% with 110 μm and 56% with 250 μm particles [33]. This excessive initial transformation is detrimental as it exhausts the material's capacity for transformation toughening, thereby limiting its ability to arrest crack propagation under subsequent functional stresses. APA with larger particles may also cause distortion of the tetragonal phase and trigger ferroelastic domain switching [43], resulting in the formation of surface irregularities and subsurface microcracks. Such defects significantly degrade the fracture strength and toughness of zirconia, potentially compromising the homogeneity and integrity of the veneering interface [16,21,22,33,44–46]. In light of this evidence, Passos et al. [21] and Kim et al. [32] advocated for APA with alumina particles no larger than 50 μm. This protocol induces optimal phase transformation while minimizing subsurface damage that could compromise material strength and interfere with the stability of the porcelain-zirconia bond.

In this study, APA significantly increased the surface roughness (R_a) for both zirconia types compared to intact surfaces (3Y-TZP: 0.28 → 0.50 μm; 4Y-TZP: 0.34 → 0.57 μm), consistent with previous reports [16,47–50]. No significant differences were observed between 3Y-TZP and 4Y-TZP after APA, although 4Y-TZP exhibited slightly higher roughness. This trend may be related to the higher yttria content of 4Y-TZP, which increases the cubic phase fraction, reduces transformation toughening, and lowers flexural strength and fracture toughness [9]. As a result, higher yttria-stabilized zirconias may exhibit a more brittle response to abrasive treatment, potentially promoting micro-fracturing and more pronounced topographical irregularities despite reduced phase transformation [10,23].

However, nanoindentation hardness and elastic modulus mapping (Fig. 2) revealed no differences between untreated and APA-treated 3Y-TZP–porcelain and 4Y-TZP–porcelain interfaces. This indicates that the phase transformation effects discussed above are not detectable at the nanoindentation scale, and that the maps primarily reflect the intrinsic mechanical contrast between zirconia and porcelain. Localized low-hardness regions observed within the porcelain layer were likely associated with voids formed during the veneering process. Nanoindentation mapping further revealed a pronounced mechanical mismatch across the zirconia–porcelain interface, with zirconia exhibiting substantially higher stiffness and hardness than porcelain. Similar gradients in elastic modulus and hardness have been reported previously and are considered critical factors influencing stress distribution and crack initiation at ceramic–ceramic interfaces [51].

To assess whether APA influenced adhesive performance, porcelain-zirconia bond strength was evaluated. APA of the zirconia substrates failed to increase the porcelain bond strength. Numerically, even lower bond strength values were observed after APA (3Y-TZP: 38.75 → 34.01 MPa; 4Y-TZP: 40.55 → 36.82 MPa). Thus, the results do not support any beneficial effect of APA on porcelain bonding. These observations are consistent with previous reports suggesting that APA does not consistently improve zirconia-veneer bonding and may not always benefit zirconia veneering when microdamage outweighs micromechanical gains [46,49,52–54]. In addition, the tetragonal-to-monoclinic transformation induced by APA in zirconia also affects the veneering porcelain due to the difference in coefficients of thermal expansion (CTE): the monoclinic phase has a CTE of 7.5 × 10^{-6}/ °C, whereas the tetragonal phase has a CTE of 10.8 × 10^{-6}/ °C [16]. Strong discrepancies in CTE between porcelain and zirconia cause the two materials to contract at considerably different rates during cooling from porcelain firing temperatures, thereby generating high residual stresses at the interface, which can lead to delamination of the porcelain from the zirconia substrate [55]. Additional heat treatment after APA has been proposed to reverse the t→m transformation and relieve compressive stresses, potentially reducing surface damage [56,57]; however, it does not repair micro-cracks [8].

In addition to surface treatment, zirconia composition has been proposed as a potential factor influencing porcelain–zirconia bond strength. To our knowledge, this is the first in vitro study to directly investigate the effect of yttria content (3Y-TZP vs. 4Y-TZP) on porcelain bonding. However, no significant differences in surface roughness or bond strength were observed between the two zirconia types, indicating that yttria content did not have a detectable impact under the conditions tested. To further explore the potential microstructural differences at the bonding interface, SEM and TEM analyses were performed, complemented by EDS line scans.

Representative micrographs revealed coherent, pore-free interfaces with relatively sharp chemical transitions between zirconia and porcelain, consistent with limited interdiffusion during porcelain firing [58,59]. However, the higher Si content detected in the zirconia bulk, exceeding the manufacturer's specified values (Table 1), may indicate diffusion of Si from the porcelain layer into the zirconia during porcelain firing. STEM–EDS further demonstrated yttrium segregation at zirconia grain boundaries, particularly in 3Y-TZP, without evidence of yttrium diffusion into the porcelain layer. Such segregation is known to influence grain-boundary chemistry, oxygen vacancy distribution, and diffusion behavior [60–62], but in this study, it did not translate into measurable differences in bond strength. Although yttrium enrichment at intergranular regions may indirectly influence interfacial bonding through effects on local stress relaxation, oxide stability, and thermal compatibility during porcelain firing, these observations support the conclusion that mechanical bonding, rather than chemical interaction, dominates the zirconia–porcelain interface.

Variations in yttria content between 3Y- and 4Y-TZP are unlikely to influence adhesive performance under standard firing and surface preparation protocols. Although the exact chemical nature of the porcelain–Y-TZP bond remains partly unclear, the minimal evidence for chemical interaction emphasizes that mechanical retention is predominant. Therefore, factors such as zirconia surface topography and the wetting properties of veneering porcelain are essential for achieving optimal bonding [63–65]. Additionally, thermal compatibility between porcelain veneers and Y-TZP ceramic cores has been identified as a crucial factor for clinical durability [66]. The low thermal conductivity of zirconia facilitates heat accumulation during cooling from firing temperatures, resulting in high residual tensile stresses at the porcelain–zirconia interface [55]. These stresses remain within the structure and may interact with functional stresses from mastication, thereby increasing the risk of porcelain delamination or chipping [67].

The observations from this study show that the effects of APA are substrate-specific: while APA enhances metal–ceramic bonding, it failed to improve the porcelain-zirconia bond strength. While the variable grain sizes between groups (50 μm for zirconia vs. 110 μm for metals)

introduce a confounding factor for direct comparison and pose a methodological limitation, this protocol was prioritized to maintain clinical relevance. Utilizing coarser particles on zirconia exhausts its transformation toughening capacity and risks structural degradation; thus, substrate-specific APA was essential to evaluate the interfaces under their respective clinically optimized conditions [21,32]. These findings collectively support a cautious approach to APA prior to porcelain veneering, aligning with manufacturer recommendations that generally advise against aggressive abrasion for zirconia to avoid surface defects and compromised bond durability [68–71].

In conclusion, the increased surface roughness (R_a) produced by APA on zirconia substrates did not result in improved porcelain bond strength compared with untreated controls, highlighting that surface roughness alone is an insufficient predictor of interfacial bonding without accounting for surface topography quality, microstructural phase composition, and potential APA-induced defects, which may play a critical role. Further, chemical bonding contributes more substantially to porcelain adhesion in metal–ceramic systems, likely explaining the higher bond strength of Co–Cr (45.54 ± 6.07 MPa), consistent with well-established clinical outcomes. This is due to the formation of a reactive, adherent oxide layer that enhances adhesion. In contrast, Ti-6Al-4V forms a brittle oxide that contributes less to bonding, and zirconia is largely chemically inert, lacking a silica-based glass phase, which limits its ability to form chemical bonds with veneering porcelain [72].

In accordance with porcelain manufacturer guidelines and established clinical protocols, different veneering porcelains were used for Co–Cr, Ti–6Al–4V, and zirconia to ensure substrate-specific compatibility in the CTE and firing conditions, minimizing interfacial residual stresses and the risk of veneer failure [34,35]. The use of different porcelains across groups introduces a confounding factor that limits direct comparison between materials and represents a methodological limitation of this study. Despite this, the approach was intentionally adopted to preserve clinical relevance and reflect real-world restorative practices.

Despite these material-dependent differences, the bond strength values recorded between dental porcelain and zirconia-based ceramics were comparable to those of the metal-ceramic systems and even slightly higher than the bond strength between dental porcelain and Ti-6Al-4V (37.33 ± 4.12 MPa). The weakest porcelain bonding was observed for Ti-6Al-4V and APA-treated zirconia substrates. In general, the strengths of the porcelain bonds to each Co-Cr, Ti-6Al-4V, 3Y-TZP, and 4Y-TZP (APA and non-APA) substrates were well above the minimal ISO 9693:2019 recommended values [30]. Accordingly, despite the recorded differences in bond strength values, all the investigated systems provide a sufficiently reliable bond for clinical application.

5. Conclusions

Within the limitations of this study, the following conclusions can be drawn:

1. The highest porcelain bond strength was observed for Co–Cr, whereas Ti–6Al–4V and APA-treated zirconia showed the lowest values; however, all tested systems exceeded the minimum bond strength requirement specified in ISO 9693:2019 and are therefore considered clinically acceptable.
2. APA increased the surface roughness of both 3Y-TZP and 4Y-TZP; however, it did not improve porcelain–zirconia bond strength.
3. Variations in yttria content in zirconia did not significantly affect porcelain–zirconia bond strength.
4. Nanoindentation and microscopic analyses revealed a pronounced mechanical mismatch and sharp, coherent interfaces between zirconia and porcelain, with yttrium segregated at grain boundaries.

CRediT authorship contribution statement

Maja Antanasova: Writing – original draft, Visualization, Methodology, Investigation, Formal analysis, Data curation, Conceptualization. **Tine Malgaj:** Writing – review & editing, Visualization, Project administration, Methodology, Data curation. **Sandra Drev:** Writing – review & editing, Visualization, Methodology. **Milan Vukšić:** Writing – review & editing, Visualization, Methodology. **Peter Jevnikar:** Writing – review & editing, Supervision, Resources, Project administration, Funding acquisition. **Andraž Kocjan:** Writing – review & editing, Supervision, Resources, Project administration, Formal analysis, Conceptualization.

Declaration of interest statement

The authors declare that they have no known competing financial interests or personal relationships that could have appeared to influence the work reported in this paper.

Acknowledgments

This work was supported by the Slovenian Research Agency funding through the research program Ceramics and complementary materials for advanced engineering and biomedical applications (P2-0087) and research project Biofunctionalization of Zirconia Abutments for Improved Peri-Implant Health: Additive Multiscale Surface Structuring Approach (BioZIR) (Z3-70130).

References

[1] F. Zarone, S. Russo, R. Sorrentino, From porcelain-fused-to-metal to zirconia: clinical and experimental considerations, Dent. Mater. 27 (2011) 83–96, https://doi.org/10.1016/J.DENTAL.2010.10.024.
[2] H.W. Roberts, D.W. Berzins, B.K. Moore, D.G. Charlton, Metal-ceramic alloys in dentistry: a review, J. Prosthodont. 18 (2009) 188–194, https://doi.org/10.1111/J.1532-849X.2008.00377.X.
[3] P. Svanborg, L. Längström, R.M. Lundh, G. Bjerkstig, A. Örtorp, A 5-year retrospective study of cobalt-chromium-based fixed dental prostheses, Int. J. Prosthodont. 26 (2013) 343–349, https://doi.org/10.11607/IJP.3024.
[4] A. Eliasson, C.F. Arnelund, A. Johansson, A clinical evaluation of cobalt-chromium metal-ceramic fixed partial dentures and crowns: a three- to seven-year retrospective study, J. Prosthet. Dent. 98 (2007) 6–16, https://doi.org/10.1016/S0022-3913(07)60032-8.
[5] M.A. Carpenter, R.J. Goodkind, Effect of varying surface texture on bond strength of one semiprecious and one nonprecious ceramo-alloy, J. Prosthet. Dent. 42 (1979) 86–95, https://doi.org/10.1016/0022-3913(79)90334-2.
[6] M. Antanasova, P. Jevnikar, Bonding of dental ceramics to titanium: processing and conditioning aspects, Curr. Oral Health Rep. 3 (2016) 234–243, https://doi.org/10.1007/s40496-016-0107-x.
[7] M. Antanasova, A. Kocjan, A. Abram, J. Kovač, P. Jevnikar, Pre-oxidation of selective-laser-melted titanium dental alloy: effects on surface characteristics and porcelain bonding, J. Adhes. Sci. Technol. 35 (19) (2021) 2094–2109, https://doi.org/10.1080/01694243.2021.1877003.
[8] I. Denry, J.R. Kelly, State of the art of zirconia for dental applications, Dent. Mater. 24 (2008) 299–307, https://doi.org/10.1016/J.DENTAL.2007.05.007.
[9] A.M. Arellano Moncayo, L. Peñate, M. Arregui, L. Giner-Tarrida, R. Cedeño, State of the art of different zirconia materials and their indications according to evidence-based clinical performance: a narrative review, Dent. J. 11 (1) (2023) 18, https://doi.org/10.3390/DJ11010018.
[10] E.A. McLaren, A. Maharishi, S.N. White, Influence of yttria content and surface treatment on the strength of translucent zirconia materials, J. Prosthet. Dent. 129 (2023) 638–643, https://doi.org/10.1016/J.PROSDENT.2021.07.001.
[11] M.F.R.P. Alves, L.Q.B. de Campos, B.G. Simba, C.R.M. da Silva, K. Strecker, C. dos Santos, Microstructural characteristics of 3Y-TZP ceramics and their effects on the flexural strength, Ceramics 5 (2022) 798–813, https://doi.org/10.3390/CERAMICS5040058.
[12] T. Mirt, A. Abram, N. van del Velde, I. Jerman, R. Bermejo, A. Kocjan, et al., Effect of airborne-particle abrasion of yttria-containing zirconia dental ceramics on mechanical properties before and after regeneration firing, J. Eur. Ceram. Soc. 42 (2022) 5035–5044, https://doi.org/10.1016/j.jeurceramsoc.2022.05.010.
[13] T. Malgaj, T. Mirt, A. Kocjan, P. Jevnikar, The influence of nanostructured alumina coating on bonding and optical properties of translucent zirconia ceramics: in vitro evaluation, Coatings 11 (2021) 1126, https://doi.org/10.3390/coatings11091126.
[14] A. Kocjan, T. Mirt, R.J. Kohal, Z. Shen, P. Jevnikar, Zirconia ceramics: clinical and biological aspects in dentistry, Encycl. Mater.: Tech. Ceram. Glas. 3 (2021) 817–832, https://doi.org/10.1016/B978-0-12-818542-1.00051-5.

[15] C. Oblak, A. Kocjan, P. Jevnikar, T. Kosmac, The effect of mechanical fatigue and accelerated ageing on fracture resistance of glazed monolithic zirconia dental bridges, J. Eur. Ceram. Soc. 37 (2017) 4415–4422, https://doi.org/10.1016/j.jeurceramsoc.2017.04.048.

[16] K. Lundberg, L. Wu, E. Papia, The effect of grinding and/or airborne-particle abrasion on the bond strength between zirconia and veneering porcelain: a systematic review, Acta Biomater. Odontol. Scand. 3 (1) (2017) 8–20, https://doi.org/10.1080/23337931.2017.1293486.

[17] M.E. Coskun, T. Akar, F. Tugut, Airborne-particle abrasion; searching the right parameter, J. Dent. Sci. 13 (2018) 293–300, https://doi.org/10.1016/J.JDS.2018.02.002.

[18] S. Bilimlerinde, D./. Sağlık, B. Değer, R. Kara, Investigation of the effect of different surface treatments on shear bond strength in the fabrication of metal-ceramic dental restorations, Value Health Sci. 12 (2022) 489–496, https://doi.org/10.33631/SABD.1172176.

[19] J. Cotič, A. Kocjan, S. Panchevska, T. Kosmač, P. Jevnikar, In vivo ageing of zirconia dental ceramics — part II: highly-translucent and rapid-sintered 3Y-TZP, Den. Mater. 37 (2021) 454–463, https://doi.org/10.1016/j.dental.2020.11.019.

[20] A. Kocjan, J. Cotič, T. Kosmač, P. Jevnikar, In vivo aging of zirconia dental ceramics – Part I: biomedical grade 3Y-TZP, Dent. Mater. 37 (2021) 443–453, https://doi.org/10.1016/j.dental.2020.11.023.

[21] S.P. Passos, B. Linke, P.W. Major, J.A. Nychka, The effect of air-abrasion and heat treatment on the fracture behavior of Y-TZP, Dent. Mater. 31 (2015) 1011–1021, https://doi.org/10.1016/J.DENTAL.2015.05.008.

[22] V. Turp, D. Sen, B. Tuncelli, G. Goller, M. Özcan, Evaluation of air-particle abrasion of Y-TZP with different particles using microstructural analysis, Aust. Dent. J. 58 (2013) 183–191, https://doi.org/10.1111/ADJ.12065.

[23] A.A. Alnazzawi, M.H. AbdElaziz, A.E. Farghal, M.F. Aldamaty, S. Borzangy, S. Ainoosah, et al., Effect of different surface treatments on the bond strength of different monolithic Zirconia with dentin, Int. Dent. J. 75 (2025) 100812, https://doi.org/10.1016/J.IDENTJ.2025.03.021.

[24] M.J. Suarez, C. Perez, J. Pelaez, C. Lopez-Suarez, E. Gonzalo, A randomized clinical trial comparing zirconia and metal-ceramic three-unit posterior fixed partial dentures: a 5-year follow-up, J. Prosthodont. 28 (2019) 750–756, https://doi.org/10.1111/JOPR.12952.

[25] F. Rathmann, M. Pohl, P. Rammelsberg, W. Bömicke, Up to 10 years clinical performance of zirconia ceramic and metal-ceramic fixed partial dentures: a retrospective study, J. Prosthet. Dent. 132 (2024) 756–765, https://doi.org/10.1016/J.PROSDENT.2022.11.003.

[26] J. Peláez, P.G. Cogolludo, B. Serrano, J.F.L. Lozano, M.J. Suárez, A prospective evaluation of zirconia posterior fixed dental prostheses: three-year clinical results, J. Prosthet. Dent. 107 (2012) 373–379, https://doi.org/10.1016/S0022-3913(12)60094-8.

[27] A. Ispas, L. Iosif, D. Popa, M. Negucioiu, M. Constantiniuc, C. Bacali, et al., Comparative assessment of the functional parameters for metal-ceramic and all-ceramic teeth restorations in prosthetic dentistry—a literature review, Biology. (Basel) 11 (2022) 556, https://doi.org/10.3390/BIOLOGY11040556.

[28] S.M. Abrisham, A. Fallah Tafti, S. Kheirkhah, M.A Tavakkoli, Shear bond strength of porcelain to a base-metal compared to zirconia core, J. Dent. Biomater. 4 (1) (2017) 367–372. PMID:28959767.

[29] L. Sreekala, M. Narayanan, S. Eerali, S. Eerali, J. Varghese, A.Z. Fathima, Comparative evaluation of shear bond strengths of veneering porcelain to base metal alloy and zirconia substructures before and after aging - an in vitro study, J. Int. Soc. Prev. Community Dent. 5 (2015) 74, https://doi.org/10.4103/2231-0762.171590.

[30] ISO 9693:2019 - Dentistry — Compatibility Testing For Metal-Ceramic and Ceramic-Ceramic Systems, International Organization for Standardization, Geneva, 2019.

[31] T. Papadopoulos, A. Tsetsekou, G. Eliades, Effect of aluminium oxide sandblasting on cast commercially pure titanium surfaces, Eur. J. Prosthodont. Restor. Dent. 7 (1) (1999) 15–21.

[32] H.-K. Kim, K.-W. Yoo, S.-J. Kim, C.-H. Jung, H.-K.;. Kim, K.-W.;. Yoo, et al., Phase transformations and subsurface changes in three dental zirconia grades after sandblasting with various Al2O3 particle sizes, Materials (Basel) 14 (2021) 5321, https://doi.org/10.3390/MA14185321.

[33] P. Łagodzińska, B. Dejak, M. Krasowski, B. Konieczny, The influence of Alumina airborne-particle abrasion with various sizes of alumina particles on the phase transformation and fracture resistance of Zirconia-based dental ceramics, Materials (Basel) 16 (2023) 5419, https://doi.org/10.3390/MA16155419.

[34] T. Korkmaz, V. Asar, Comparative evaluation of bond strength of various metal–ceramic restorations, Mater. Des. 30 (2009) 445–451, https://doi.org/10.1016/J.MATDES.2008.06.002.

[35] S.C. Lopes, V.O. Pagnano, J.M.D. De Almeida Rollo, M.B. Leal, O.L. Bezzon, Correlation between metal-ceramic bond strength and coefficient of linear thermal expansion difference, J. Appl. Oral Sci. 17 (2009) 122–128, https://doi.org/10.1590/S1678-77572009000200010.

[36] M. Antanasova, A. Kocjan, M. Hočevar, P. Jevnikar, Influence of surface airborne-particle abrasion and bonding agent application on porcelain bonding to titanium dental alloys fabricated by milling and by selective laser melting, J. Prosthet. Dent. 123 (2020) 491–499, https://doi.org/10.1016/J.PROSDENT.2019.02.011.

[37] M. Antanasova, A. Kocjan, J. Kovač, B. Žužek, P. Jevnikar, Influence of thermo-mechanical cycling on porcelain bonding to cobalt–chromium and titanium dental alloys fabricated by casting, milling, and selective laser melting, J. Prosthodont. Res. 62 (2) (2018) 184–194, https://doi.org/10.1016/j.jpor.2017.08.007.

[38] M. Antanasova, A. Kocjan, A. Abram, J. Kovač, P. Jevnikar, Pre-oxidation of selective-laser-melted titanium dental alloy: effects on surface characteristics and porcelain bonding, J. Adhes. Sci. Technol. 35 (2021) 2094–2109, https://doi.org/10.1080/01694243.2021.1877003.

[39] L. Audi, A. Al-mustafa, Bending strength and hardness comparison of titanium and cobalt–chromium alloys for dentures made by selective laser melting, Sci. Rep. 15 (2025) 36463, https://doi.org/10.1038/S41598-025-21191-3.

[40] B. Yilmaz, S. Ayyildiz, U.T. Kalyoncuoglu, A. Tahmasebifar, E.T. Baran, Surface characteristics of additively manufactured CoCr and Ti6Al4V dental alloys: the effects of carbon and gold thin film coatings, and alkali-heat treatment, Microsc. Res. Tech. 87 (2024) 1222–1240, https://doi.org/10.1002/JEMT.24501.

[41] P. Shelar, S. Butler, H. Abdolvand, On the behaviour of zirconia-based dental materials: a review, J. Mech. Behav. Biomed. Mater. 124 (2021) 104861, https://doi.org/10.1016/J.JMBBM.2021.104861.

[42] I.A. Ciobotaru, M. Stoicanescu, R. Budei, A. Cojocaru, D.I. Vaireanu, Considerations regarding sandblasting of Ti and Ti6Al4V used in dental implants and abutments as a preconditioning stage for restorative dentistry works, Appl. Sci. (Switzerland) 14 (2024) 7365, https://doi.org/10.3390/APP14167365/S1.

[43] R.H.J. Hannink, P.M. Kelly, B.C. Muddle, Transformation toughening in zirconia-containing ceramics, J. Am. Ceram. Soc. 83 (2000) 461–487, https://doi.org/10.1111/j.1151-2916.2000.tb01221.x.

[44] L. Hallmann, P. Ulmer, E. Reusser, C.H.F. Hämmerle, Effect of blasting pressure, abrasive particle size and grade on phase transformation and morphological change of dental zirconia surface, Surf. Coat. Technol. 206 (2012) 4293–4302, https://doi.org/10.1016/J.SURFCOAT.2012.04.043.

[45] F. Zicari, C. Monaco, V. Cardoso, M.;. Silvestri, S. Carossa, S.L. Iconaru, et al., Bonding effectiveness of veneering ceramic to zirconia after different grit-blasting treatments, Dent. J. 12 (2024) 219, https://doi.org/10.3390/DJ12070219.

[46] T. Kosmač, C. Oblak, P. Jevnikar, N. Funduk, L. Marion, The effect of surface grinding and sandblasting on flexural strength and reliability of Y-TZP zirconia ceramic, Dent. Mater. 15 (1999) 426–433, https://doi.org/10.1016/S0109-5641(99)00070-6.

[47] V. Vilas Boas Fernandes Júnior, D.C. Barbosa Dantas, E. Bresciani, M.F Rocha Lima Huhtala, Evaluation of the bond strength and characteristics of zirconia after different surface treatments, J. Prosthet. Dent. 120 (2018) 955–959, https://doi.org/10.1016/J.PROSDENT.2018.01.029.

[48] H.J. Kim, H.P. Lim, Y.J. Park, M.S. Vang, Effect of zirconia surface treatments on the shear bond strength of veneering ceramic, J. Prosthet. Dent. 105 (2011) 315–322, https://doi.org/10.1016/S0022-3913(11)60060-7.

[49] A. Nishigori, T. Yoshida, M.C. Bottino, J.A. Platt, Influence of zirconia surface treatment on veneering porcelain shear bond strength after cyclic loading, J. Prosthet. Dent. 112 (2014) 1392–1398, https://doi.org/10.1016/J.PROSDENT.2014.05.029.

[50] P. Łagodzińska, B. Dejak, B. Konieczny, The influence of Alumina airborne-particle abrasion on the properties of zirconia-based dental ceramics (3Y-TZP), Coatings 13 (2023) 1691, https://doi.org/10.3390/COATINGS13101691.

[51] I.-C. Pang, J.L. Gilbert, J. Chai, E.P. Lautenschlager, Bonding characteristics of low-fusing porcelain bonded to pure titanium and palladium-copper alloy, J. Prosthet. Dent. 73 (1995) 17–25.

[52] H. Onuma, M. Inokoshi, K. Xu, S. Minakuchi, Fracture strength of porcelain veneer on surface-treated zirconia, Dent. Mater. J. 43 (2024) 263–268, https://doi.org/10.4012/DMJ.2023-139.

[53] M. Doi, K. Yoshida, M. Atsuta, S. Takahashi, Influence of pre-treatments on flexural strength of zirconia and debonding crack-initiation strength of veneered zirconia, J. Adhes. Dent. 13 (1) (2011) 79–84, https://doi.org/10.3290/J.JAD.A18239.

[54] G. Wang, S. Zhang, C. Bian, H. Kong, Effect of zirconia surface treatment on zirconia/veneer interfacial toughness evaluated by fracture mechanics method, J. Dent. 42 (2014) 808–815, https://doi.org/10.1016/J.JDENT.2014.04.005.

[55] N. Juntavee, C. Dangsuwan, Role of coefficient of thermal expansion on bond strength of ceramic veneered yttrium-stabilized zirconia, J. Clin. Exp. Dent. 10 (2018) 0, https://doi.org/10.4317/JCED.54605.

[56] D. Liu, J.P. Matinlinna, J.K.H. Tsoi, E.H.N. Pow, T. Miyazaki, Y. Shibata, et al., A new modified laser pretreatment for porcelain zirconia bonding, Dent. Mater. 29 (2013) 559–565, https://doi.org/10.1016/J.DENTAL.2013.03.002.

[57] O. Kirmali, H. Akin, A.K. Ozdemir, Shear bond strength of veneering ceramic to zirconia core after different surface treatments, Photomed. Laser. Surg. 31 (2013) 261–268, https://doi.org/10.1089/PHO.2013.3487.

[58] J. Fischer, P. Grohmann, B. Stawarczyk, Effect of zirconia surface treatments on the shear strength of zirconia/veneering ceramic composites, Dent. Mater. J. 27 (2008) 448–454, https://doi.org/10.4012/DMJ.27.448.

[59] C.M. Ramos, P.F. Cesar, R.F. Lia Mondelli, A.S. Tabata, J. De Souza Santos, A. F Sanches Borges, Bond strength and Raman analysis of the zirconia-feldspathic porcelain interface, J. Prosthet. Dent. 112 (2014) 886–894, https://doi.org/10.1016/J.PROSDENT.2014.02.009.

[60] R.L. González-Romero, J.J. Meléndez, Yttrium segregation and oxygen diffusion along high-symmetry grain boundaries in YSZ, J. Alloys. Compd. 622 (2015) 708–713, https://doi.org/10.1016/J.JALLCOM.2014.10.184.

[61] O.G. Licata, M. Zhu, J. Hwang, B. Mazumder, Nanoscale chemistry and ion segregation in zirconia-based ceramic at grain boundaries by atom probe tomography, Scr. Mater. 213 (2022) 114603, https://doi.org/10.1016/J.SCRIPTAMAT.2022.114603.

[62] K. Matsui, H. Yoshida, Y. Ikuhara, Grain-boundary segregation and phase-separation mechanism in Yttria-stabilized tetragonal zirconia polycrystal, Key. Eng. Mater. 484 (2011) 82–88, https://doi.org/10.4028/WWW.SCIENTIFIC.NET/KEM.484.82.

[63] M.N. Aboushelib, N. De Jager, C.J. Kleverlaan, A.J. Feilzer, Microtensile bond strength of different components of core veneered all-ceramic restorations, Dent. Mater. 21 (2005) 984–991, https://doi.org/10.1016/J.DENTAL.2005.03.013.

[64] M.N. Aboushelib, C.J. Kleverlaan, A.J. Feilzer, Microtensile bond strength of different components of core veneered all-ceramic restorations. Part II: zirconia veneering ceramics, Dent. Mater. 22 (2006) 857–863, https://doi.org/10.1016/J.DENTAL.2005.11.014.
[65] N.Z. Fahmy, Bond strength, microhardness, and core/veneer interface quality of an all-ceramic system, J. Prosthodont. 19 (2010) 95–102, https://doi.org/10.1111/J.1532-849X.2009.00540.X.
[66] J.B.C. Meira, B.R. Reis, C.B. Tanaka, R.Y. Ballester, P.F. Cesar, A. Versluis, et al., Residual stresses in Y-TZP crowns due to changes in the thermal contraction coefficient of veneers, Dent. Mater. 29 (2013) 594–601, https://doi.org/10.1016/J.DENTAL.2013.03.012.
[67] K.A. Fukushima, M.J. Sadoun, P.F. Cesar, A.K. Mainjot, Residual stress profiles in veneering ceramic on Y-TZP, alumina and ZTA frameworks: measurement by hole-drilling, Dent. Mater. 30 (2014) 105–111, https://doi.org/10.1016/J.DENTAL.2013.10.005.
[68] M. Falahchai, H. Neshandar Asli, M. Faghani, A. Hendi, Effect of different surface treatments on shear bond strength of zirconia with various yttria contents, BMC Oral Health 24 (2024) 1520, https://doi.org/10.1186/S12903-024-05348-6.
[69] D. Shen, H. Wang, Y. Shi, Z. Su, M. Hannig, B. Fu, The effect of surface treatments on zirconia bond strength and durability, J. Funct. Biomater. 14 (2) (2023) 89, https://doi.org/10.3390/JFB14020089.
[70] F.V. Martins, W.F. Vasques, G.H. Guyatt, E.M. Fonseca, Effect of aluminum oxide airborne-particle abrasion on zirconia bond strength to tooth or composite resin substrates: a systematic review and meta-analysis, J. Prosthet. Dent. 135 (2) (2026) 278.e1–278.e16, https://doi.org/10.1016/J.PROSDENT.2025.09.020.
[71] Ivoclar Vivadent A.G. ZirCAD Labside: instructions for use [Internet]. Rev. 3. Schaan (Liechtenstein): ivoclar Vivadent AG; 2019 [cited 2026 Mar 16]. Available form: https://ivodent.hu/_docs/879_d22d71ac6f0f520972113de4bae74b42.pdf.
[72] S.G. Mihali, A. Hiller, State-of-the-art zirconia and glass–Ceramic materials in restorative dentistry: properties, clinical applications, challenges, and future perspectives, Appl. Sci. 15 (2025) 12841, https://doi.org/10.3390/APP152312841.